Method to remove the effect of ambient temperature on radiometric calibration

Chang Songtao,[1,2,*] Zhang Yaoyu,[1] Sun Zhiyuan,[1] and Li Min[1]

[1]Changchun Institute of Optics, Fine Mechanics and Physics, Chinese Academy of Sciences, Changchun 130033, China

[2]University of Chinese Academy of Sciences, Beijing 100039, China

*Corresponding author: stchang2010@sina.com

Received 18 July 2014; revised 15 August 2014; accepted 15 August 2014;
posted 18 August 2014 (Doc. ID 217232); published 18 September 2014

High precision radiometric calibration is essential for infrared imaging systems, especially in scientific applications where an accurate quantitative analysis is required. Nevertheless, calibration and radiometry are usually not simultaneously performed. Hence the discrepancy of ambient temperature between calibration and actual measurement can generate significant measurement errors unless the calibration results have been properly corrected. To overcome the restriction, we studied the effect of ambient temperature on radiometric calibration, then derived the relationship between calibration results and ambient temperature considering the integration time. A novel method compensating for the impact of ambient temperature on the calibration of a cooled infrared system is proposed. Several experiments are performed, and the results indicate that the proposed method can not only ensure the accuracy of calibration but achieve calibration results under any ambient temperature and arbitrary integration time. © 2014 Optical Society of America

OCIS codes: (040.2480) FLIR, forward-looking infrared; (040.3060) Infrared; (010.5630) Radiometry; (120.6810) Thermal effects; (290.2648) Stray light.

http://dx.doi.org/10.1364/AO.53.006274

1. Introduction

With the development of infrared detectors and radiometry technology, infrared imaging systems are widely used to measure the radiation characteristics of military and scientific objects. However, underexposure or saturation of the detector limits the dynamics of the resolvable incident irradiance. To overcome this restriction and achieve high dynamic range radiometry, several different integration times are selected [1,2]. As a result, reference sources at various levels of radiance are needed for radiometric calibration. Due to the complexity of such sources as well as of the handling of these sources, a considerable time may be needed for the calibration, which tends to become impractical in radiometry tasks with time limitations. Always there is a considerable time lag between calibration and radiometry due to time and condition limitations of field trials. For example, the infrared imaging system may be calibrated in the laboratory rather than in the field, hence the ambient temperature differences in calibration and measurement process. Besides, the ambient temperature varies during a long duration radiometry. As is known, ambient temperature fluctuations will certainly cause output drift of an infrared system. The drift not only restricts the precision of radiometry but leads to nonuniformity of the output image. As a consequence, it is meaningful to study the effect of ambient temperature on radiometric calibration results at different integration times.

A number of papers and patents that address the problem above have been published in recent years, and the approaches are briefly classified into three categories. (1) Due to the effect of ambient temperature fluctuations, the infrared system has to be frequently recalculated during a radiometry task if

1559-128X/14/276274-06$15.00/0
© 2014 Optical Society of America

the accuracy is to be maintained. Hence it is extremely important to reduce the time of calibration. Ochs *et al.* proposed a pixel-wise calibration method which achieves high dynamic range by using fewer reference sources [1]. This method has the advantage of yielding a high radiometric accuracy, whereas its drawbacks lie in the fact that each time a new calibration is required, the detector's normal operation needs to be interrupted. Moreover it tends to become impractical for high dynamic range radiometry and real-time applications. (2) To avoid frequent calibration, it is effective to maintain the accuracy by temperature control methods which keep the ambient temperature constant. However, this approach is mainly used in infrared telescopes rather than typical infrared imaging systems, for the quite high cost and difficulties of implementation. (3) For infrared systems with cooled detectors, the effect of ambient temperature mainly results from stray radiation. Stray radiation is commonly analyzed by programs such as Zemax; however, the results are mainly used in optic design and infrared system evaluation rather than radiometry [3–5]. The reason lies in its significant error, compared with real conditions, caused by ideal treatments of materials, bidirectional reflectance distribution function (BRDF), and characteristics of the lens.

In this article, radiometric calibration formulas considering integration time are proposed, and the impact of ambient temperature on calibration is analyzed in Section 2. Following this, a method to remove the effect of ambient temperature fluctuations on calibration at arbitrary integration times is proposed in Section 3. Then calibration experiments are carried out to verify the theories described above in Section 4. It is concluded in Section 5 that our method yields high precision while allowing the user to perform radiometric calibration in the laboratory before radiometry; thus the detector's normal operation does not need to be interrupted by repeated calibrations in field trials. Besides, it improves the efficiency of high dynamic range calibration and radiometry and gives users the freedom of optimizing the detector output to the current scenery.

2. Effect of Ambient Temperature on Infrared Imaging System

A. Radiometric Calibration Considering the Integration Time

Radiometric calibration of an infrared imaging system is essential to properly determine the target's radiance or temperature. Infrared systems, in many applications, are operated in a range of irradiance within which detectors exhibit linear input–output characteristics. In this paper we adopt the near-extended-source method for calibration at a preselected integration time [6–8]. The output gray value [digital number (DN)] is given by the approximate linear relation:

$$h_{i,j} = G_{i,j} \cdot L_t + B_{i,j}, \tag{1}$$

where $h_{i,j}$ is the gray value of the (i,j)th detector in the array, $G_{i,j}$ is the response associated with radiance of the reference source, and $B_{i,j}$ is the offset. The radiance L_t can be calculated by

$$L_t = \varepsilon \cdot L(T_t) = \frac{\varepsilon}{\pi} \int_{\lambda_1}^{\lambda_2} M(\lambda, T_t) \mathrm{d}\lambda, \tag{2}$$

where $L(T_t)$ denotes the in-band radiance of an ideal blackbody at the same absolute temperature T_t as the reference source. $\lambda_1 \sim \lambda_2$ is the integration range, and $M(\lambda, T_t)$ is the spectral radiant excitance of an ideal blackbody calculated by Planck's formula. The geometry of calibration is illustrated in Fig. 1.

The radiation flux received by a detector element is

$$\Phi_t = \frac{\pi \cdot \varepsilon \tau_{\mathrm{opt}}}{4} \cdot \left(\frac{D}{f}\right)^2 \cdot A_d \cdot L(T_t) = k_t L(T_t), \tag{3}$$

where τ_{opt} denotes transmittance of the optics, D denotes the diameter of the optics, f is the focal length, and A_d is sensitive area of a detector element; hence $k_t = (\pi \cdot \varepsilon \tau_{\mathrm{opt}}/4)(D/f)^2 A_d$ is constant for a given infrared system. The response of a detector element to incident flux is therefore given by $G'_{i,j} = G_{i,j}/k_t$. The offset $B_{i,j}$, originating from the reflected ambient radiation, stray radiation, and internal factors of the detector, for instance dark current, that strike the detector element, is given by

$$B_{i,j} = G'_{i,j} \cdot \Phi_{b,i,j} + G'_{i,j} \cdot \Phi_{\mathrm{sys},i,j} + h_{\mathrm{det},i,j}, \tag{4}$$

where $\Phi_{b,i,j}$ is the reflected ambient radiation flux, $\Phi_{\mathrm{sys},i,j}$ is the stray radiation flux, and $h_{\mathrm{det},i,j}$ is the gray value offset caused by internal factors of the detector. $\Phi_{b,i,j}$ and $\Phi_{\mathrm{sys},i,j}$ are obviously in relation to the ambient temperature. However, for a cooled infrared system, where the temperature of the detector elements keeps almost constant (i.e., 77 K), $h_{\mathrm{det},i,j}$ is assumed to be independent of the ambient temperature.

In order to meet high dynamic range requirements of imaging as well as radiometry applications, infrared imaging systems are usually calibrated at several different integration times. Of course, $G'_{i,j} \cdot$

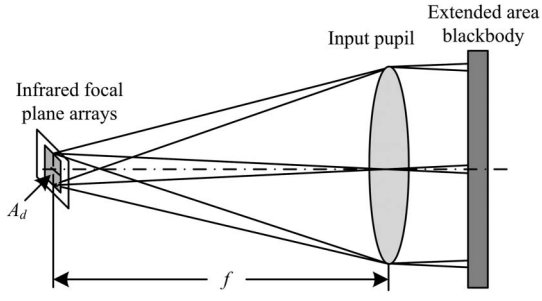

Fig. 1. Schematic diagram of radiometric calibration using extended area blackbody.

$\Phi_{b,i,j}$ and $G'_{i,j} \cdot \Phi_{\mathrm{sys},i,j}$ are proportional to the integration time as long as the incident radiation flux falls into the linear range of detector response [9,10]. Furthermore, since the output gray value is linear to the integration time, $h_{\mathrm{det},i,j}$ should also be linear to the integration time, such that

$$h_{\mathrm{det},i,j}(t) = t \cdot h_{\mathrm{det}\,1,i,j} + h_{\mathrm{det}\,2,i,j}. \tag{5}$$

Ignoring the index of the detector element above, Eq. (1), namely the calibration formula, can be rewritten as

$$h = t \cdot G'(\Phi_t + \Phi_{\mathrm{sys}} + \Phi_b) + t \cdot h_{\mathrm{det}\,1} + h_{\mathrm{det}\,2}, \tag{6}$$

where t is the integration time in units of milliseconds; G' therefore is redefined as the normalized radiation flux response in units of DN/(W·s). It is noticed that, for the near-extended-source calibration method, the reference source is so close to the detector that the atmospheric effects, namely absorption and scattering, can be ignored.

B. Effect of Ambient Temperature on Calibration

Experiments illustrated that the output gray value drifts when the ambient temperature changes. To compensate the effect of gray value drift on calibration, we studied the sources that generate it. Cooled infrared detectors are known to work at a stabilized temperature, so the response of detectors would not vary with the ambient temperature. If the temperature of the reference source stays constant, the drift originates from stray radiation of the infrared imaging system, reflected ambient radiation, and internal factors of the detector.

Stray radiation, for a well-designed infrared imaging system, mainly results from radiation of the lens, radiation of the housing cone and other mechanical structures, and the narcissus signature. The narcissus signature is radiation of the cooled detector that reflected by the optics; in other words the detector sees its own image. It can be weakened by reducing the reflectivity of the core surfaces. Noticing that the narcissus, for an optical system with fixed lens and other components, is independent of the ambient temperature; we subsume it into $h_{\mathrm{det}}(t)$ for simplification. However, the radiation of the lens and other components is determined by their own temperature. Due to their thermal conductivity, the temperature of the components turns to became uniform. In this paper, all the components are assumed to be at the ambient temperature except for the detector and its surroundings [3,4].

We first consider the stray radiation seen by a single detector element (i,j), assuming that an element area ds emits a very small solid angle of a stray light bundle, which is finally seen by the detector element through some optical paths, where there may be transmitting, reflecting, absorbing, scattering, or any composition of these [3]. Figure 2 shows the transmission path of stray radiation in detail.

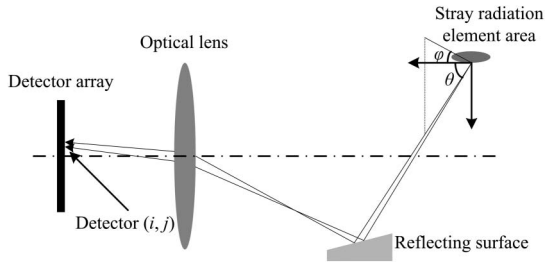

Fig. 2. Geometry of stray radiation.

The radiation flux of ds that reaches detector (i,j) is given by

$$d\Phi_{\mathrm{sys}} = \varepsilon(\theta,\varphi) \cdot L(T_{\mathrm{amb}}) \cdot ds \cdot \Omega \cdot \tau \cdot \rho, \tag{7}$$

where $\varepsilon(\theta,\varphi)$ is the emissivity of ds in direction (θ,φ), the temperature of ds is equal to T_{amb}, Ω denotes the projected solid angle, τ is the transmittance of the bundle from ds to detector (i,j), and ρ is the path reflectance. The total radiation flux emitted from the lens and other components that strikes the detector element (i,j) is given by

$$\Phi_{\mathrm{sys}}(T_{\mathrm{amb}}) = \sum_{i=1}^{n} \varepsilon(\theta_i,\varphi_i) \cdot L(T_{\mathrm{amb}}) \cdot s_i \cdot \Omega_i \cdot \tau_i \cdot \rho_i, \tag{8}$$

where n is the number of the element areas that propagate to the detector, and s_i is the area of the ith element. Denoting $\sum_{i=1}^{n} \varepsilon(\theta_i,\varphi_i) \cdot s_i \cdot \Omega_i \cdot \tau_i \cdot \rho_i$ by k_{sys}, Eq. (8) can be simplified as

$$\Phi_{\mathrm{sys}}(T_{\mathrm{amb}}) = k_{\mathrm{sys}} \cdot L(T_{\mathrm{amb}}). \tag{9}$$

Since k_{sys} is constant in theory for a given infrared system, the flux resulting from stray radiation of the system is directly proportional to the radiance of an ideal blackbody at ambient temperature.

The reflected ambient radiation flux denoted by Φ_b can be expressed as

$$\Phi_b = \frac{\pi(1-\varepsilon)\tau_{\mathrm{opt}}}{4}\left(\frac{D}{f}\right)^2 \cdot A_d \cdot L(T_{\mathrm{amb}}) = k_b L(T_{\mathrm{amb}}), \tag{10}$$

where $k_b = (\pi(1-\varepsilon)\tau_{\mathrm{opt}}/4)(D/f)^2 \cdot A_d$ is constant for a given infrared system. Equation (10) indicates that the flux Φ_b is also directly proportional to $L(T_{\mathrm{amb}})$. Substituting Eq. (9) and Eq. (10) into Eq. (6), we obtain

$$h(t,T_{\mathrm{amb}}) = t \cdot G' k_t L_t(T_t) + t \cdot G'(k_{\mathrm{sys}} + k_b) L(T_{\mathrm{amb}}) + t \cdot h_{\mathrm{det}\,1} + h_{\mathrm{det}\,2}. \tag{11}$$

3. Removing the Effect of Ambient Temperature on Calibration

According to Eq. (11), $h(t,T_{\mathrm{amb}})$ is linear to the integration time t as long as the ambient temperature is stabilized. Therefore, the calibration formula at an

arbitrary integration time can be determined given the calibration results at two different integration times. In order to analyze the effect of ambient temperature on calibration at an arbitrary integration time, we assume that the infrared imaging system is calibrated at two integration times, namely t_0 and t_1, and the ambient temperature is T_{amb0}. The calibration results are as follows:

$$h(t_0, T_{\text{amb0}}) = t_0 \cdot G' k_t L_t(T_t) + t_0 \cdot G'(k_{\text{sys}} + k_b) L(T_{\text{amb}}) + t_0 \cdot h_{\text{det1}} + h_{\text{det2}}, \tag{12}$$

$$h(t_1, T_{\text{amb0}}) = t_1 \cdot G' k_t L_t(T_t) + t_1 \cdot G'(k_{\text{sys}} + k_b) L(T_{\text{amb}}) + t_1 \cdot h_{\text{det1}} + h_{\text{det2}}. \tag{13}$$

Thereupon the calibration result at an arbitrary integration time namely t can be represented as:

$$h(t, T_{\text{amb0}}) = \frac{t - t_0}{t_1 - t_0} \cdot h(t_1, T_{\text{amb0}}) + \frac{t_1 - t}{t_1 - t_0} \cdot h(t_0, T_{\text{amb0}}). \tag{14}$$

However, if the ambient temperature changes, to T_{amb} for example, the calibration should be updated to maintain the accuracy of radiometry. It can be discovered from Eq. (11) that the stray radiation changes while the ambient temperature increases (reduces) from T_{amb0} to T_{amb}, such that

$$\begin{aligned} \Delta h &= h(t, T_{\text{amb}}) - h(t, T_{\text{amb0}}) \\ &= t \cdot G' \cdot (k_{\text{sys}} + k_b) \cdot [L(T_{\text{amb}}) - L(T_{\text{amb0}})]. \end{aligned} \tag{15}$$

Assuming the integration time is set as t_0 while the ambient temperature changes from T_{amb0} to T_{amb}, we obtain

$$G' \cdot (k_{\text{sys}} + k_b) = \frac{h(t_0, T_{\text{amb1}}) - h(t_0, T_{\text{amb0}})}{t_0 \cdot [L(T_{\text{amb1}}) - L(T_{\text{amb0}})]}. \tag{16}$$

Submitting Eq. (16) to Eq. (15) yields

$$\Delta h = \frac{t}{t_0} \cdot \frac{L(T_{\text{amb}}) - L(T_{\text{amb0}})}{L(T_{\text{amb1}}) - L(T_{\text{amb0}})} [h(t_0, T_{\text{amb1}}) - h(t_0, T_{\text{amb0}})]. \tag{17}$$

Thus,

$$\begin{aligned} h(t, T_{\text{amb}}) &= h(t, T_{\text{amb0}}) + \Delta h \\ &= \frac{t - t_0}{t_1 - t_0} \cdot h(t_1, T_{\text{amb0}}) + \frac{t_1 - t}{t_1 - t_0} \cdot h(t_0, T_{\text{amb0}}) \ldots . \\ &\quad + \frac{t}{t_0} \cdot \frac{L(T_{\text{amb}}) - L(T_{\text{amb0}})}{L(T_{\text{amb1}}) - L(T_{\text{amb0}})} [h(t_0, T_{\text{amb1}}) \\ &\quad - h(t_0, T_{\text{amb0}})]. \end{aligned} \tag{18}$$

Equation (18) indicates that it is possible to obtain calibration results at an arbitrary integration time and ambient temperature if calibration results, namely $h(t_0, T_{\text{amb0}})$, $h(t_1, T_{\text{amb0}})$, and $h(t_0, T_{\text{am10}})$, are obtained previously. The calibration at arbitrary integration time can be updated, in order to remove the effect of ambient temperature fluctuations, by adding Δh to the calibration result at the original ambient temperature, namely T_{amb0}. The calibration therefore is not required to be performed frequently in radiometry or imaging applications. Besides, for high dynamic range infrared imaging systems, only two integration times are needed to obtain the calibration results of arbitrary integration time, which can naturally reduce the complexity of calibration devices and the time that calibration requires.

4. Experimental Results

To verify the theories described above, experiments were performed with a mid-wave infrared (MWIR) camera of forward looking infrared (FLIR) systems having a large-scale mercury cadmium telluride (MCT) focal plane array (FPA) (640 × 512 pixels). The camera operates in the 3.7–4.8 μm waveband, with a 14-bit digital output. The extended area blackbody selected as the reference source has a 100 mm × 100 mm size and exhibits high effective emissivity (0.97 in the 3.7–4.8 μm waveband). Its temperature accuracy is 0.01°C over an operating temperature range of 0°C–125°C. The experimental setup used for radiometric calibration is sketched in Fig. 3.

In order to control the ambient temperature of the infrared imaging system, we place the whole system including the camera and the blackbody into a chamber and change the temperature inside from 0°C to 50°C. Experiments indicate that the temperature inside will be stabilized in a few minutes once the chamber's temperature is set, and the accuracy is ±0.2°C. In order to evaluate the performance of the calibration correction method proposed in this paper, several calibration experiments are carried out in the chamber. They are performed in four steps:

(1) The ambient temperature is originally set to 10°C, namely T_{amb0}. Then the infrared imaging system is calibrated looking at the reference source at temperature 40°C and 50°C, and the integration times are selected as 1 and 2 ms.

(2) The ambient temperature is then set to 20°C and the infrared imaging system is calibrated at integration time of 1 ms.

(3) According to the calibration results above, the output gray value drift caused by ambient

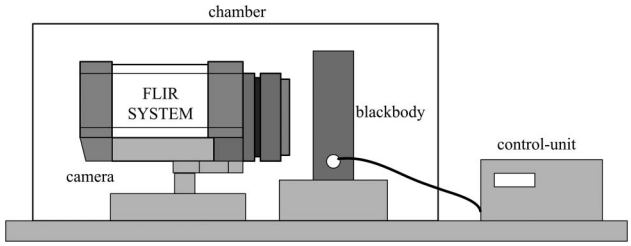

Fig. 3. Experimental setup for calibration.

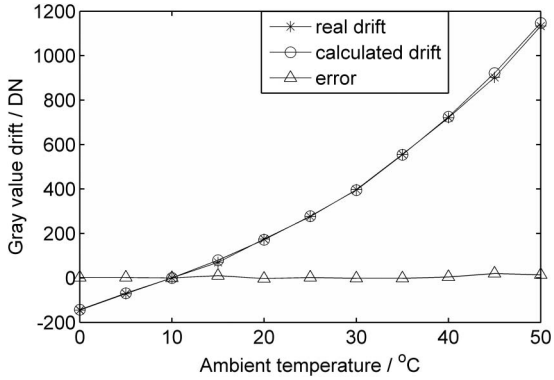

Fig. 4. Calculated gray value drifts compared with the real ones at 2 ms.

temperature fluctuations can be calculated using Eq. (17). Besides, Eq. (18) demonstrates that the effect of ambient temperature fluctuations on calibration results at arbitrary integration time can be removed, which means that we can update the calibration results by calculation instead of performing the calibration frequently.

(4) The integration times 0.5 and 2 ms are selected, for example, to verify the theories in this paper. The calibrations are performed at the ambient temperature varying from 0°C to 50°C, with 5°C as the interval. To verify the calibration correction method proposed, another experiment is performed at several integration times, namely 0.2, 0.5, 0.8, 1, 1.2, 1.5, 1.8, and 2 ms, under a certain ambient temperature, namely 40°C.

We define the differences between gray values at different ambient temperatures with that of 10°C as the real output gray value drifts that are caused by ambient temperature fluctuations. The calculated gray value drifts at 0.5 and 2 ms are compared with the real ones. As is shown in Fig. 4, the calculated drifts are approximate to the real ones, which demonstrates that Eq. (17) is valid for our infrared imaging system.

In order to test the accuracy of our calibration correction method, an experiment as presented in step (4) is performed. We define the original calibration error as the error caused by ignoring the effect of

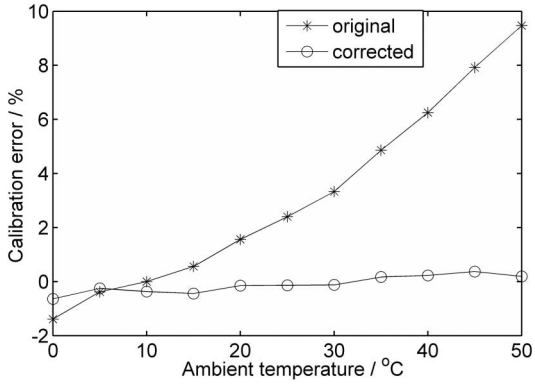

Fig. 5. Calibration error as a function of ambient temperature at 0.5 ms.

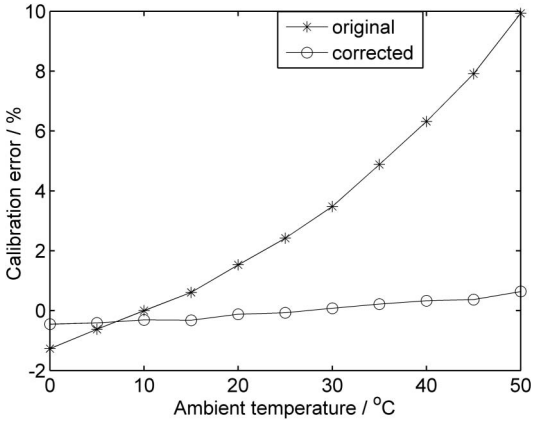

Fig. 6. Calibration error as a function of ambient temperature at 2 ms.

ambient temperature fluctuations, which also means taking the calibration result at T_{amb0} as the result of other ambient temperatures. As is known, the original calibration error, which may lead to significant radiometry error, appears in many applications. The calibration correction method in this paper aims to compensate the calibration error caused by ambient temperature fluctuations. Therefore, the results are compared with the original calibration error in order to evaluate the effectiveness.

It is illustrated in Figs. 5 and 6 that the original calibration error increases when the ambient temperature rises. As is shown in Figs. 5 and 6, the maximum error reaches nearly 10%, which is unacceptable for IR system in scientific applications. After correction, the calibration error is limited to 0.64%, which demonstrates that the method in this paper yields high accuracy of calibration under various ambient temperatures. Figure 7 shows the calibration error for various integration times under a certain ambient temperature. After correction, the calibration error reduces greatly, which illustrates that the calibration correction method proposed in this paper is valid for arbitrary integration time. In summary, the method proposed in this paper, yielding high accuracy of calibration at arbitrary integration time and ambient temperature, is valid for our infrared imaging system.

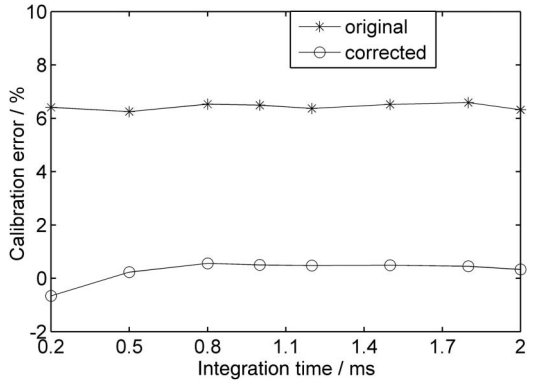

Fig. 7. Calibration error at several integration times.

5. Conclusion

This paper introduces an approach to compensate for the effect of ambient temperature fluctuations on radiometric calibration. By analyzing the calibration considering the integration time as well as the effect of ambient temperature on the output gray value, the calibration formula considering the integration time and ambient temperature is deduced. Then the gray value drifts, and calibration results at arbitrary integration time and ambient temperature are calculated by the theory proposed in this paper. Finally, calibration experiments are performed in a chamber with controllable inside temperature to evaluate whether the method proposed is effective for our infrared system. Experimental results illustrate that the calibration correction method yields high precision of calibration and gives the user the freedom to optimize the detector output to the current scenery by changing the integration time.

The main advantages of the approach developed in this paper are as follows: (1) the detector's normal operation does not need to be interrupted by repeated calibration; (2) the infrared imaging system is simplified, thus saving cost and benefitting the operator; and (3) it improves the efficiency of high dynamic range radiometric calibration and measurement, as well as gives the user the freedom to optimize the detector output to the current scenery.

References

1. M. Ochs, A. Schulz, and H.-J. Bauer, "High dynamic range infrared thermography by pixelwise radiometric self calibration," Infrared Phys. Technol. **53**, 112–119 (2010).
2. T. Svensson and I. Renhorn, "Evaluation of a method to radiometric calibrate hot target image data by using simple reference sources close to ambient temperature," Proc. SPIE **7662**, 76620X (2010).
3. E. C. Fest, *Stray Light Analysis and Control* (SPIE, 2013).
4. Y. Liu, X.-Q. An, and Q. Wang, "Accurate and fast stray radiation calculation based on improved backward ray tracing," Appl. Opt. **52**, B1–B9 (2013).
5. F. Marcotte, P. Tremblay, and V. Farley, "Infrared camera NUC calibration: comparison of advanced methods," Proc. SPIE **8706**, 870603 (2014).
6. M. D. Mermelstein, K. A. Snail, and R. G. Priest, "Spectral and radiometric calibration of midwave and longwave infrared cameras," Opt. Eng. **39**, 347–352 (2000).
7. W. L. Wolfe, *Introduction to Radiometry* (SPIE, 1998).
8. G. C. Holst, *Testing and Evaluation of Infrared Imaging Systems* (JCD, 1933).
9. X. Sui, Q. Chen, and G. Gu, "Nonuniformity correction of infrared images based on infrared radiation and working time of thermal imager," Optik **124**, 352–356 (2013).
10. Y. Jin, J. Jiang, and G. Zhang, "Three-step nonuniformity correction for a highly dynamic intensified charge-coupled device star sensor," Opt. Commun. **285**, 1753–1758 (2012).